FATIGUE BEHAVIOR OF RECTANGULAR BUILT-UP HOLLOW SECTION JOINT MADE OF HIGH STRENGTH STEEL S690

M.S. Zhao[*†], S.P. Chiew and C.K. Lee

School of Civil and Environmental Engineering, Nanyang Technological University, Singapore

ABSTRACT:

Structural Hollow Sections (SHS), especially rectangular sections, are widely used in welded steel frames for their advantages in both efficiency and aesthetics, and its popularity is still growing rapidly. Recently, some newly developed low alloy quenched and tempered high strength structural steels have attracted more and more attention due to higher strength to weight ratio and lower cost compared with traditional alloy high strength steel or work hardened steels. However, the use of such high strength steel is still questionable in some non-strength dominating conditions, such as fatigue. This study looked into the potential fatigue issues of built-up rectangular hollow section joints made of reheated, quenched and tempered high strength steel S690. Experimental investigations were carried out to study such joints' fatigue behavior at both high stress ratio and low stress ratio state. Three dimensional cyclic loadings, i.e. axial force, in-plane bending and out-plane bending, were applied to generate the fatigue loading. The stress concentration factors (SCF) around the intersection were measured by strain gauges method. Subsequently, the fatigue tests were launched under the supervision of the alternative current potential drop (ACPD) crack monitoring system. Test results were verified by comparing with available literature and common fatigue design standards. It was found out that the built-up hollow sections were the same as traditional hot rolled or cold-formed hollow sections in transferring the loading from brace to chord, and high strength steel hollow section joints were not different from mild steel hollow section joints in fatigue resistance.

Keywords: Fatigue, high strength steel, hollow section joints, stress concentration factor.

1. INTRODUCTION

Quenched and tempered low alloy structural steel plate (QT steel), the most common high strength steel, develop their high strength from complex heat-treatments, rather than rely merely on more alloy elements (Bhadeshia et al. 2006). Heat treatment grants steels better performance in yield / tensile strength without sacrificing weldability compared with the other type of high strength steel, the high alloy steels. Currently, the design standards for structural steel buildings such as ANSI/AISC 360-05 (AISC 2005) and EN1993-1 (EC3 2005) clearly allow the application of high strength quenched and tempered steel with yield strength up to 690MPa. However, the use of quenched and tempered high strength in off-shore structures, one of the most important application for high strength steels, is still questionable since the dominating problem in the area, fatigue, cares much more than just strength, e.g. size and geometric parameters of the structures (Lee et al. 2005; Schumacher et al. 2009), residual stress (Ohta et al. 1986; Zamiri et al. 2012), stress ratio (Chen et al. 1992; Sakai et al. 2006) and loading conditions (Seto et al. 2007). This study looked into the potential fatigue issues of built-up rectangular hollow section joints made of reheated, quenched and tempered high strength steel S690. Experimental investigations were carried out to study these

[*] Corresponding author: Email: mzhao1@ntu.edu.sg

[†] Presenter: Email: mzhao1@ntu.edu.sg

joints' fatigue behavior at both high stress range ratio and low stress range ratio state. Three dimensional cyclic loadings, i.e. axial force, in-plane bending and out-plane bending, were applied at the brace end to generate the fatigue loading. The stress concentration factors (SCF) around the intersection were measured by quadratic strain gauges method. Subsequently, the fatigue tests were launched under the supervision of the alternative current potential drop (ACPD) crack monitoring system. Finally, test results were verified by comparing with prediction S-N curves by CIDECT.

2. SCOPE OF TEST, SETUP AND SPECIMEN DETAILS

The experimental investigation for the high strength steel hollow section T joints was carried out in two phases. First, static loads in three directions (axial force, in-plane bending and out-plane bending) were applied on the brace end to measure the hot spot stresses (HSS) stress concentration factors (SCF). Second, combined sinusoidal loads were applied at the brace end until fatigue failure, and the results were validated against the UK DEN S-N curves (Zhao et al. 2000). During the cyclic loading phase, crack initiation and propagation were monitored and recorded by ACPD system.

2.1 Material

The research target in this project, reheated, quenched and tempered (RQT) structural steel plates, have nominal yield strength of 690 N/mm^2, and tensile strength between 790 N/mm^2 and 930 N/mm^2. As the product of a reformed quenching and tempering technique, RQT steel plates acquired more uniform and stable mechanical properties through thickness compared with traditional direct quenched and tempered steels. These RQT steel plates comply with the EN 10025-6 grade S690 specification (BSI 2004), which is approximately equivalent to the ASTM A514 steel (ASTM 2009). The mechanical properties of RQT-S690 at room temperature acquired from standard tensile test are shown in Table 1.

Table 1 The mechanical properties of RQT-S690

Strengths	$f_{0.2,n}$	$f_{2.0,n}$	$f_{u,n}$	E_n	Elongation
RQT-S690	769.0	817.1	849.8	201.3	13%

2.2 Specimen and test setup

The studied square hollow section T joints were fabricated from RQT-S690 steel plates by welding. The weld profiles and specimen preparation were carried out according to AWS structure welding Code (AWS 2008). The fabrication consists of two steps. First step was cutting the plates into long strips and forming them into rectangular hollow sections, i.e. building the hollow sections. Second, the brace section was welded onto the surface of the chord section to form the T joints, i.e. assembling the joints. The welding configurations in both steps are shown in Figure 1, while the global geometrical parameters of the joints are listed in Table 2.

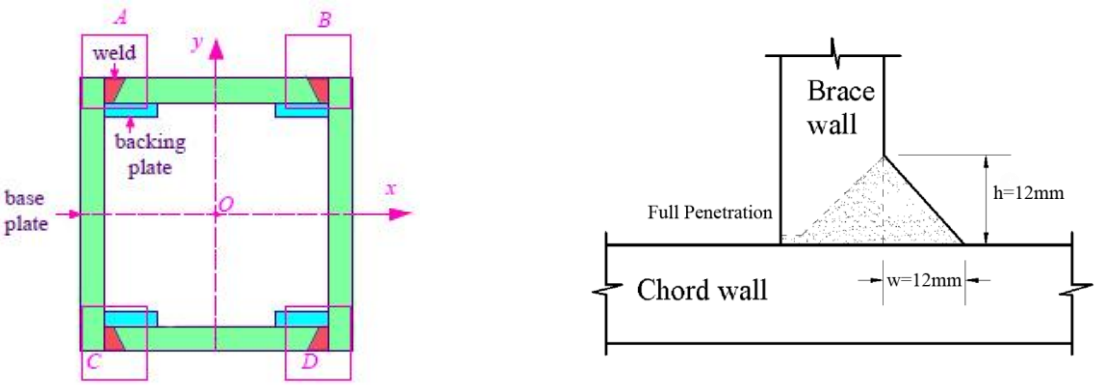

Figure 1 The fabrication procedures for the built-up square hollow section joints

In this study, a specially designed test rig that could apply axial (AX), in-plane bending (IPB) and out-plane bending or any combination of these basic load was used to test the hollow section T joints. This rig was capable of applying static loads for static test that determines the stress concentration factors (SCF) and hot spot stress (HSS) as well we cyclic dynamic loads to investigate the fatigue lives and fracture behaviors after crack appeared. To generate the three dimensional loads, independent actuators, i.e. actuator AX, actuator IPB and actuator OPB were installed on each direction. Actuator AX and IPB have maximum capacity of 250KN while Actuator OPB has 150KN.

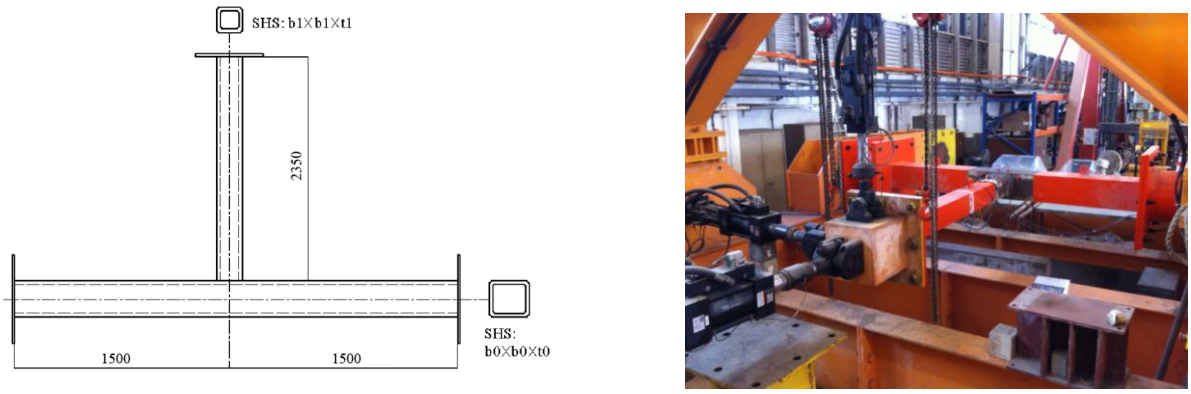

Figure 2 Specimen and the loading frame

Table 2 Specimen geometry details

Specimen	b_o (mm)	t_o (mm)	b_1 (mm)	t_1 (mm)	$\beta = \frac{b_1}{b_0}$	$2\gamma = \frac{b_0}{t_0}$	$\tau = \frac{t_1}{t_0}$
	300	12	200	12	0.667	25	1.0

3. PHASE I: STATIC TEST

3.1 Strain gauge system in static test

Strain gauges were arranged around the brace-to-chord intersections on both joints to capture the hot spot strain distribution. As the strain distribution near the weld toe is highly non-linear, the quadratic perpendicular strain / stress extrapolation method was used to measure SCF. three strain gauges were arrayed at each location along the line perpendicular to the weld toe at distances equal

to 0.4t, 0.9t and 1.4t (t is the thickness of the chord or brace), which followed the CIDECT SCF capturing guide (Zhao et al. 2000). For Specimens-I, 40 sets of strain gauge were(Withers et al. 2008) installed on the chord side, and there were 20 sets on brace side. Based on the result of specimen-I, strain gauge numbers were reduced for specimen-II. 28 sets of strain gauges were installed on the chord side, and 20 sets on brace side. The locations of the strain gauges are marked with the angle α in this paper, as shown in Figure 3. Besides, there were 9 sets of strain gauges on the mid span of the brace (3 on each face) to capture the nominal stress / strain.

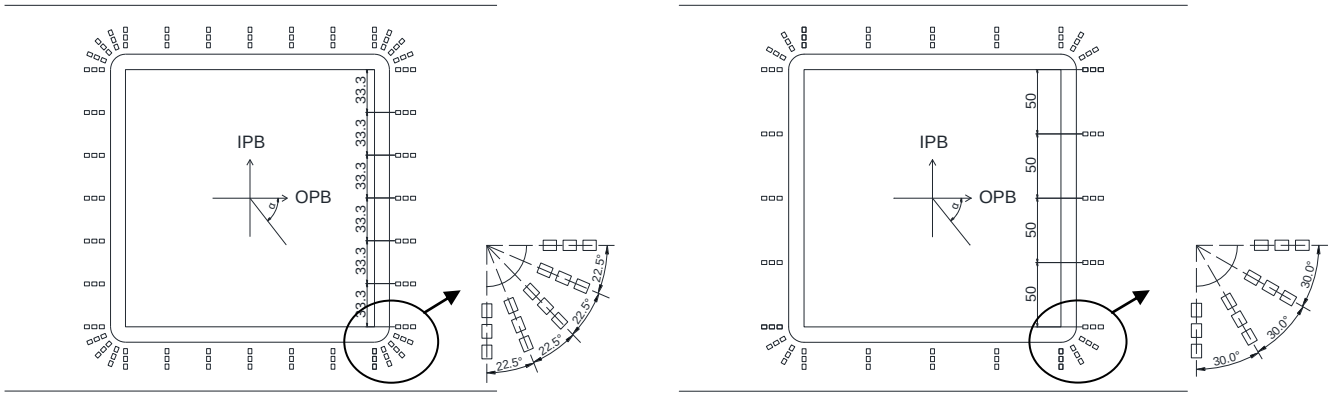

Figure 3 Strain gauges locations for specimen-I (left) and specimen-II (right)

3.2 Static test procedure

Single direction loads were applied to the specimens to check the SCFs under simple loads. The strain readings were analyzed and the hot spot strain (HSSN) was obtained using the quadratic extrapolation method for strains on chord side and linear extrapolation method for strains on brace side. The strain concentration factor (SNCF) is calculated as

$$SNCF = \frac{HSSN}{SN_{nominal}} \tag{1}$$

where $SN_{nominal}$ is the nominal strain recorded by the strain gauges at the mid span of the brace. Assuming that the measured strains $\xi_{\perp}$ and $\xi_{\parallel}$ are, respectively, the maximum and minimum principal strains at the weld toe, the corresponding SCF can be computed as

$$SCF = SNCF \frac{(1 + v\xi_{\parallel} / \xi_{\perp})}{(1 - v^2)} = SNCF \times SSCF \tag{2}$$

where v=0.3 is the poisons' ratio and SSCF is the stress-strain conversion factor. SSCF here adopted the proposed value 1.1 (Dutta 1996). Test results show that SCFs at brace side were much smaller than those at chord side, while the values were close to those of mild steel rectangular hollow section joints (Chiew et al. 2007). Besides, high symmetry corresponding to geometry could be observed in the distribution of SCF, and stresses tended to concentrate at corners. The SCF distribution of AX, IPB and OPB on the chord side of Specimen-I are presented in Figure 4 for instance.

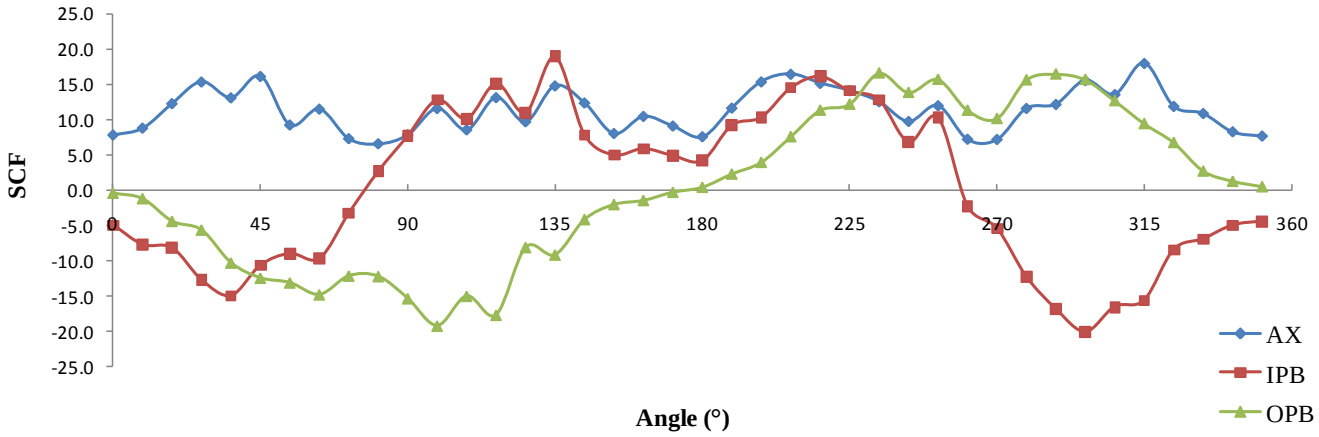

Figure 4 SCF distribution around the chord of specimen-I

Based on the theory of superposition method for SCF (Chiew et al. 2004), the stress at a given point (p) under any combined load cases can be calculated as,

$$\sigma_{(p)} = SCF_{AX(p)} \times \sigma_{n-AX} + SCF_{IPB(p)} \times \sigma_{n-IPB} + SCF_{OPB(p)} \times \sigma_{n-OPB} \quad (3)$$

where $SCF_{AX(p)}$, $SCF_{IPB(p)}$ and $SCF_{OPB(p)}$ are, respectively, the SCFs at point p for the AX IPB and OPB loads; σ_{n-AX}, σ_{n-IPB} and σ_{n-OPB} are the corresponding nominal stresses. This study checked the validity of Eq. (3) by comparing the test result under certain load with the computed corresponding results by Eq.(3). Examples using a load case of AX=120KN, IPB=4KN and OPB=4KN for specimen-I, and AX=70KN, IPB=1.0 KN and OPB=3.6KN for Specimen-II are shown in Figure 5. As the stress distribution obtained by the superposition method agreed excellently with the experimental measurement data in all the combined load cases, it is confirmed that the superposition method can be applied to high strength QT steel rectangular hollow section joints.

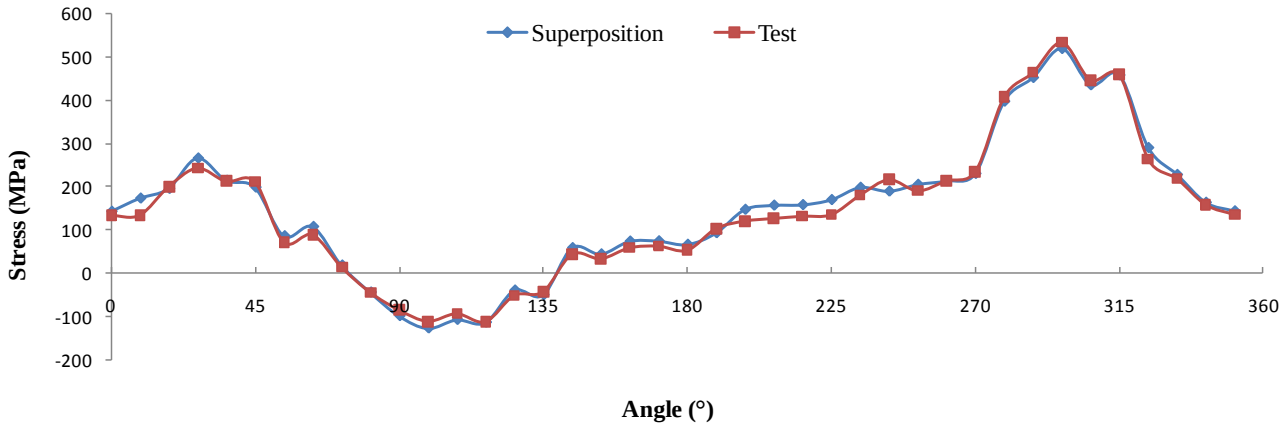

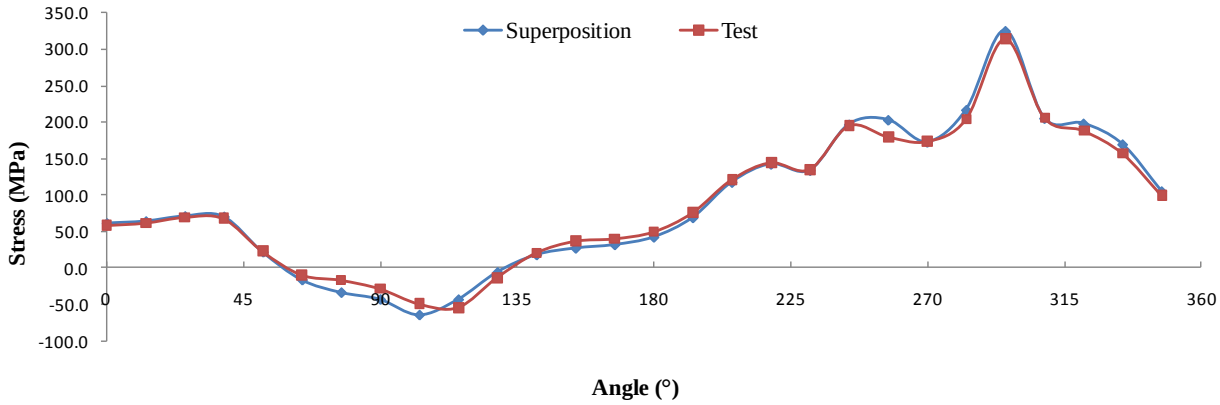

Figure 5 Comparison between test and superposition method (Specimen-I: above; Specimen-II: below)

4. PHASE 2: FATIGUE TEST

4.1 Monitoring system

The Alternating Current Potential Drop technique (Lugg 2008) was used in the cyclic fatigue test to monitor and record the crack initiation and further propagation. Based on the peak hot spot stress locations acquired from the static test, 32 sets of probes were installed around the chord-brace intersections, as shown in Figure 6. The probes were placed at equal intervals of 10mm along the weld toe, i.e. in total the monitored length was 320mm.

Figure 6 The ACPD system installed on the joints

4.2 Applied fatigue loads

Both specimens were tested in air under sinusoidal constant amplitude loadings cases that are the combination of three basic loading until fatigue crack penetrated the thickness thoroughly. The cyclic loading cases applied to both specimens are listed in Table 3. As there was zero load at the minimum stress state, the corresponding hot spot stress range distributions are the same as the maximum stress state, as shown in Figure 5.

Table 3 The fatigue load applied to the T joints

	Specimen-I (KN)	Specimen-II (KN)
AX	$AX = 60 \pm 60\sin\theta$	$AX = 60 \pm 60\sin\theta$
IPB	$IPB = -2 \pm 2\sin\theta$	$IPB = 0.5 \pm 0.5\sin\theta$
OPB	$OPB = 2 \pm 2\sin\theta$	$OPB = 1.8 \pm 1.8\sin\theta$

4.3 Fatigue test results

Specimen-I was tested under high stress state, i.e. maximum stress range equals to 69.6% of the 0.2% strain offset yield strength, while specimen-II was under low stress state with stress ratio of 42.3%. The initiation and propagation paths of both specimens were surprisingly the same, i.e. initiating at the peak hot spot stress range position and propagate in both direction but mainly along the OPB direction, as shown in Figure 7. The fatigue life before crack initiation is defined as the period between the first load cycle and N_2, the cycle that crack can be detected visually (by ACPD herein, i.e. $depth \approx 0.3\,\text{mm}$). Figure 8 shows the plot the test results of both specimens against the design S-N curve by CIDECT (Zhao et al. 2000). The fatigue life of specimen-II was slightly lower than the predicted life, while the life of Specimen-I was higher than the predicted. Therefore, it could be concluded that the quenched and tempered steel rectangular hollow section joints have advantages over mild steel joints at high stress range state, but was no better than mild steel at low stress range state.

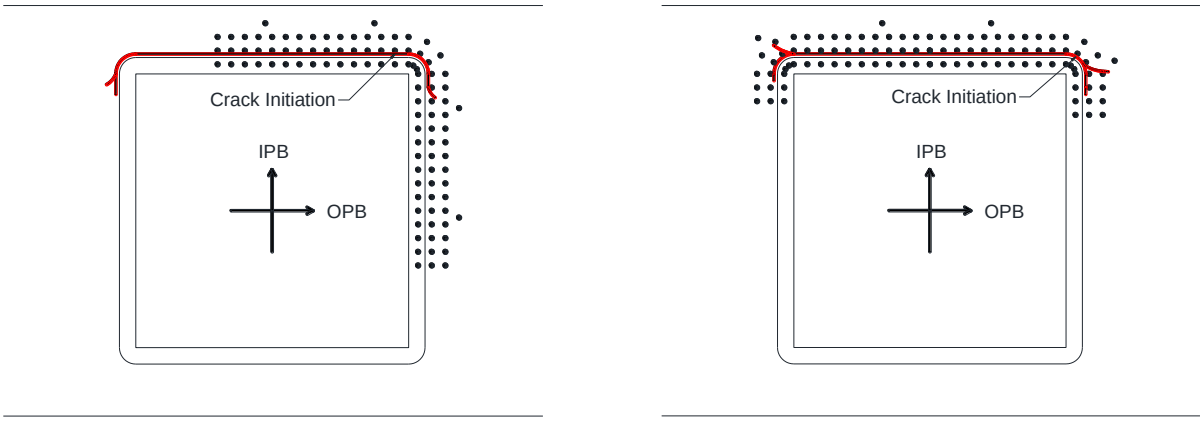

Figure 7 Crack profiles of Specimen-I (left) and Specimen-II (right)

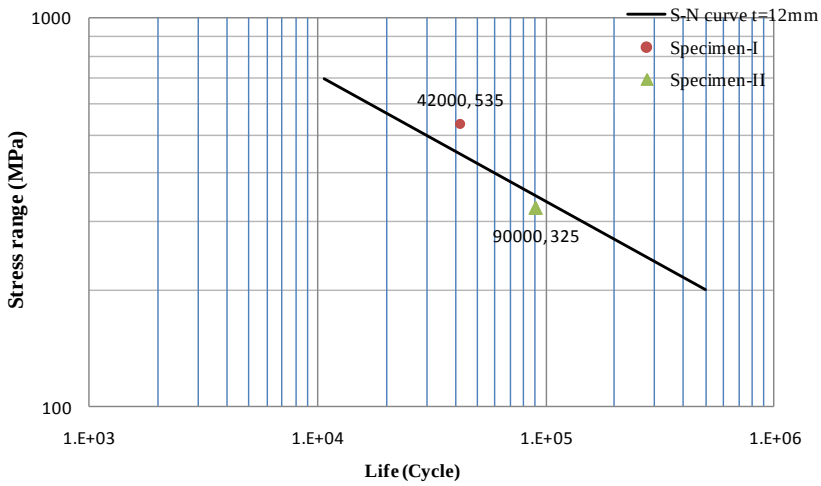

Figure 8 Test results versus SN-curve

5. CONCLUSIONS

Fatigue tests were carried out to investigate the behavior of two built-up hollow section joints made of quenched and tempered high strength steel plates. Combined load cases including AX, IPB and OPB direction loads were applied to test the specimens. Test results indicated that all the traditional fatigue life measurement methods were applicable for the built-up section joints. By comparing the

test results with CIDECT guide, it could be concluded that the behavior of both specimens was quite similar to mild steel rectangular hollow section joints, despite that RQT-S690 joint showed better fatigue resistance at high stress range state. Roughly, CIDCT guide was capable of predicting the fatigue lives of such joints.

REFERENCES

AISC (2005). Specification for structural steel buldings. ANSI/AISC 306-05. Chicago, Americal Institute of Steel Construction.

ASTM (2009). Standard specification for High-Yield-Strength, Quenched and Tempered Alloy Steel Plate, Suitable for Welding, ASTM International.

AWS (2008). Structural Welding Code. steel. Miami, American National Standards Institue.

H. K. D. H. Bhadeshia and R. W. K. Honeycombe (2006). Steels: microstructure and properties, Elsevier Ltd.

BSI (2004). Hot rolled Products of structural steels. Part6: Technical delivery conditions for flat products of high yield strength structural steels in the quenched and tempered condition. London, British Standards Institution.

D. L. Chen, B. Weiss and R. Stickler (1992). "Effect of stress ratio and loading condition on the fatigue threshold." International Journal of Fatigue 14(5): 325-329.

S. P. Chiew, C. K. Lee, S. T. Lie and H. L. Ji (2007). "Fatigue behaviors of square-to-square hollow section T-joint with corner crack. I: Experimental studies." Engineering Fracture Mechanics 74(5): 703-720.

S. P. Chiew, S. T. Lie, C. K. Lee and Z. W. Huang (2004). "Fatigue performance of cracked tubular T-joints under combined loads - Part I experimental." J Stuct Engng(130(4)): 562-571.

D. Dutta (1996). Parameters influencing the stress concentration factors in joints in offshore structures. Fatigue in offshore structures. A. A. Balkema. Rotterdam. 1: 77-128.

EC3 (2005). Eurocode 3: Design of steel structures. part 1-1: General rules and rules for buildings.

C. K. Lee, L. S. Tjhen, C. S. Ping and S. Yongbo (2005). "Numerical models verification of cracked tubular T, Y and K-joints under combined loads." Engineering Fracture Mechanics 72(7): 983-1009.

M. C. Lugg (2008). ACPD User Manual. Milton Keynes, UK, Technical Software Consultants Ltd.

A. Ohta, Y. Maeda, T. Mawari, S. Nishijima and H. Nakamura (1986). "Fatigue strength evaluation of welded joints containing high tensile residual stresses." International Journal of Fatigue 8(3): 147-150.

T. Sakai, Y. Sato, Y. Nagano, M. Takeda and N. Oguma (2006). "Effect of stress ratio on long life fatigue behavior of high carbon chromium bearing steel under axial loading." International Journal of Fatigue 28(11): 1547-1554.

A. Schumacher, L. C. Borges and A. Nussbaumer (2009). "A critical examination of the size effect correction for welded steel tubular joints." International Journal of Fatigue 31(8–9): 1422-1433.

A. Seto, T. Yamamoto and T. Niwa (2007). "Influences of loading direction and thickness ratio on fatigue properties of tailored welded blanks." International Journal of Fatigue 29(4): 729-737.

P. J. Withers, M. Turski, L. Edwards, P. J. Bouchard and D. J. Buttle (2008). "Recent advances in residual stress measurement." International Journal of Pressure Vessels and Piping 85(3): 118-127.

F. Zamiri, A. Nussbaumer and C. Acevedo (2012). Numerical investigation of welding residual stresses in plannar bridge trusses made of CHS steel profiles. Tubular Structures XIV. L. Gardner, Taylor & Francis Group: 219-225.

X. Zhao, S. Herion, J. Packer, R. Puthli, G. Sedlacek and J. Wardenier (2000). "Design guide for circular and rectangular hollow section joints under fatigue loading." CIDECT, TUV Germany.